GEOPHYSICAL RESEARCH LETTERS, VOL. 35, L18201, doi:10.1029/2008GL034954, 2008

Temperature response of Mars to Milankovitch cycles

Norbert Schorghofer[1]

Received 7 June 2008; accepted 14 August 2008; published 23 September 2008.

[1] On Mars annual mean surface temperature near ±60° latitude varies predominately with precession and is not closely related to annual mean insolation. Based on the last few million years of orbital history, the precession cycle dominates in a narrow latitude range 54°–65°, in which the margins of the two ice-rich permafrost layers in each hemisphere happen to lie, while mean annual temperature at other latitudes is controlled by the obliquity cycle. The phenomenon already exists on an airless uniform body in Mars orbit, where this latitude range shifts to 62°–74° on both hemispheres, and is closely related to temperature amplitude dependent reradiation into space. **Citation:** Schorghofer, N. (2008), Temperature response of Mars to Milankovitch cycles, *Geophys. Res. Lett.*, *35*, L18201, doi:10.1029/2008GL034954.

[2] The periodic nature of the Polar Layered Deposits of Mars has long led to speculations about orbital climate forcing [e.g., *Murray et al.*, 1973; *Toon et al.*, 1980; *Laskar et al.*, 2002]. Mars also possesses tropical mountain glaciers and, the largest ice reservoir by area, ice-rich permafrost; shallowly buried water ice exists poleward of about 60° on both hemisphere of Mars [*Boynton et al.*, 2002; *Feldman et al.*, 2002; *Mitrofanov et al.*, 2002], and, irrespective of how it has been emplaced, its extent is controlled by atmospheric humidity and annual mean surface temperature [*Mellon and Jakosky*, 1993; *Schorghofer*, 2007a]. By conservation of mass, any change in ice volume must be reflected in more than one reservoir. With the discovery [*Boynton et al.*, 2002; *Feldman et al.*, 2002; *Mitrofanov et al.*, 2002] and theoretical understanding [*Leighton and Murray*, 1966; *Mellon and Jakosky*, 1993; *Schorghofer*, 2007b] of these vast permafrost regions it is possible to investigate changes in ice extent in response to external climate forcing, as Adhémar, Croll, Milankovitch, and others have done for Earth [*Imbrie and Imbrie*, 1979]. One component of this astronomical theory [*Toon et al.*, 1980; *van Hemelrijck*, 1983; *Ward*, 1992] is the relation between orbital changes and surface temperature variations.

[3] The orbital elements of Mars are known to about 20 Ma into the past [*Laskar et al.*, 2004], and although ultimately chaotic [*Touma and Wisdom*, 1993] they evolve in an almost quasi-periodic manner analogous to the Milankovitch cycles of Earth. Insolation is affected by the planet's axis tilt (obliquity) θ, the eccentricity e of the orbit around the sun, and the longitude of the perihelion ω measured from the planet's moving equinox. Mars' orbital eccentricity varies with a period of 95 ka; the precession period is 51 ka, and the obliquity changes with a 120 ka periodicity, with additional periods longer than one million years [*Ward*, 1974, 1979, 1992]. The Fourier amplitudes for Earth and Mars are shown in Figure 1 to compare not only periodicities but also amplitudes. The obliquity of Mars varies much more than Earth's; over the last 3 Ma, obliquity oscillated around a value of 25° with extremes of 15° and 35°, but reached values beyond 45° more than 5 Ma ago when precipitation occurred in the tropics [*Forget et al.*, 2006].

[4] It has been demonstrated that the extent of the permafrost on Mars is controlled by vapor exchange between the atmosphere and the shallow subsurface [*Mellon et al.*, 2004; *Schorghofer and Aharonson*, 2005; *Diez et al.*, 2008], irrespective of whether the ice was emplaced by precipitation or diffusion. The stability boundary, which dictates the geographic extent of the permafrost, depends on the annual mean surface temperature T_m and the frost point temperature T_f which characterizes the atmospheric humidity,

$$T_f = T_m + \mathcal{C}. \tag{1}$$

The temperature difference $\mathcal{C}$ is caused by saturation of the atmosphere at night. Simple theoretical estimates yield $\mathcal{C} \sim 5$ K [*Schorghofer*, 2007a]. Figure 2 shows the relation between T_f and T_m from detailed equilibrium model calculations by *Schorghofer and Aharonson* [2005] where $\mathcal{C} \sim 7$ K. Either way, T_f and T_m vary, while $\mathcal{C}$ may be considered a constant.

[5] The relation between insolation and temperature is in principle much simpler for the martian climate system than for Earth's. On Mars lateral heat transfer in the tenuous atmosphere is small. Surface temperatures can be obtained from a one-dimensional thermal balance between incoming solar light and reradiation from the surface to space with simple approximations of atmospheric absorption and emission [*Kieffer et al.*, 1977]. Mars' atmosphere consists predominately of CO_2 that partially freezes out in winter and forms a seasonal CO_2 cover; this is also incorporated in the model. An important parameter is the thermal inertia I of the soil, which describes the temperature change due to heat input and mainly depends on soil thermal conductivity.

[6] Figure 3 shows annual mean surface temperatures for the last 5 Ma at several northern hemisphere latitudes. At polar latitudes the temperature depends strongly on obliquity; at the equator temperature varies less but is still dominated by the obliquity period. Remarkably, mean annual surface temperature varies comparatively little at 60°N. Whether the correspondence between this temperature variability minimum and the ice stability boundary is a coincidence is not immediately clear. The mean annual surface temperature at 60°N has a root-mean-square variation of only 2 K. Because T_m varies so little there, T_f is a crucial parameter for the extent of the two permafrost layers.

[7] Moreover the dominant periodicity at 60° is not the 120 ka obliquity cycle, but the 51 ka precession cycle.

[1] Institute for Astronomy, University of Hawaii at Manoa, Honolulu, Hawaii, USA.

0094-8276/08/2008GL034954$05.00

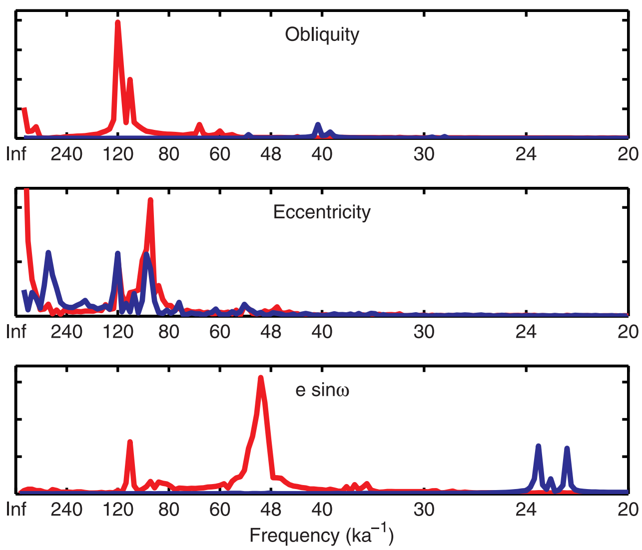

Figure 1. Fourier amplitudes of obliquity, eccentricity, and $e \sin \omega$ using the last 3 Ma of orbital history of Mars (red) and Earth (blue).

Precession, unlike obliquity, affects the two hemispheres asymmetrically. Over the last 20 ka, T_m at 60°N has increased (Figure 3) and at 60°S it has decreased, which may cause an asymmetry in the water cycle.

[8] Figure 4 reveals dependencies of T_m on orbital elements (compare with Figure 1). At most latitudes, obliquity dominates the variability over the last 3 Ma, but at 60°N it is the precession cycle. Annual mean insolation completely fails to reveal how annual mean surface temperature depends on orbital elements at 60°N. Mean annual temperature is not only determined by mean annual insolation because the outgoing radiative heat loss depends on surface temperature amplitude.

[9] The calculations in Figure 3 are for a planet with uniform thermal properties and thus without the influence of the ice on thermal properties of the soil. Model calculations with zonally averaged thermal properties and subsurface ice produce close to the same results. Model calculations without seasonal CO_2 cover also show a minimum in variability although it is less pronounced. The minimum is still present on a planet without atmosphere, and therefore a variability minimum already exists on a uniform airless spherical body.

[10] The instantaneous incoming solar flux Q depends on heliocentric distance and solar incidence angle. The mean annual insolation at latitude φ is given by [*Ward*, 1974]

$$\overline{Q} = \frac{1}{2\pi^2} \frac{S}{\sqrt{1-e^2}} \int_0^{2\pi} \sqrt{1 - (\sin\varphi\cos\theta - \cos\varphi\sin\theta\sin\psi)^2} d\psi, \tag{2}$$

where S is the solar constant at Mars semimajor axis, θ obliquity, and ψ an integration variable. The annual mean is independent of the longitude of the perihelion, and it depends on eccentricity only beyond first order. A corollary of this fact is that variation in $\overline{Q}$ is dominated by obliquity changes.

[11] Mean annual insolation can be viewed as an end-member model where the surface remains at constant temperature. This equilibrium temperature T_{eq} is determined by $(1\text{-}A)\ \overline{Q} = \varepsilon\sigma\ T_{eq}^4$, where A is albedo, ε infrared emissivity, and σ the Stefan-Boltzmann constant. For small obliquity the integrand in equation (2) can be expanded in a Taylor series and integrated to yield

$$\overline{Q} = \frac{1}{\pi} \frac{S}{\sqrt{1-e^2}} \left[1 + \frac{\tan^2\varphi - 1}{4}\theta^2 + O(\theta^4)\right] \cos\varphi. \tag{3}$$

From this expression it is apparent that the dependence on obliquity almost vanishes at latitudes of $\varphi = \pm 45°$, a variability minimum that parallels that in T_m.

[12] The other end-member extreme is represented by an instantaneous equilibration of surface temperature [*Rubincam*, 2004]. It is commonly used for asteroids and in this context known as "standard thermal model" [*Lebofsky and Spencer*, 1990]. Its surface temperature is set by $(1\text{-}A)\ Q = \varepsilon\sigma T_{st}^4$. The average surface temperature $\overline{T_{st}}$ is thus given by $\overline{Q^{1/4}}$. Fourier transforms reveal that $\overline{Q^{1/4}}$ varies mainly with the precessional period everywhere except near the equator. It is remarkable that a 10° variation in obliquity has less influence on $\overline{T_{st}}$ than a change in eccentricity by 0.1. This can be readily understood at the extremes of the poles where insolation varies greatly with obliquity yet $\overline{T_{st}}$ varies primarily with precession. The time averaged $Q^{1/4}$ weighs small values of Q more than large values of Q and is thus sensitive to the length of seasons and insensitive to peak insolation. This makes plausible the dominance of the precession period.

[13] A quantitative calculation supports this argument. At the north pole, Q is proportional to $\sin\theta \sin(\nu + \omega)$ when $Q > 0$, where ν is the angle between perihelion and the position of the sun. The time-averaged moment is $\overline{Q^{1/4}} = \frac{1}{P}\int_{-\omega}^{\pi-\omega} Q^{1/4} \frac{dt}{d\nu} d\nu$, where P is the orbital period. The

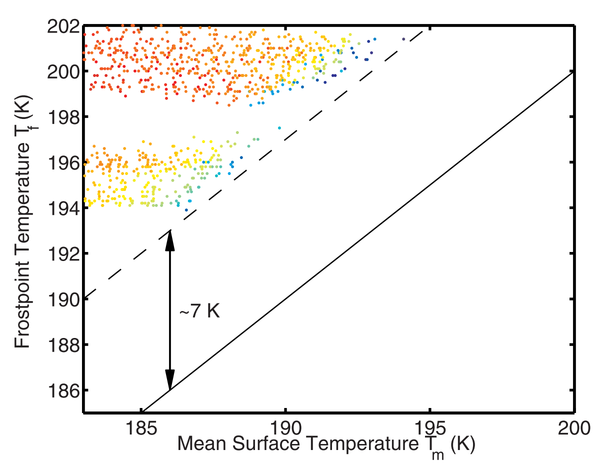

Figure 2. Temperature and humidity in areas where ice is stable according to equilibrium model calculations [*Schorghofer and Aharonson*, 2005]. Colors indicate the depth of the equilibrium ice table, with blue being deep and red being shallow. The solid black line shows $T_f = T_m$. The data fall into two groups because the atmosphere in the southern hemisphere is drier than in the north.

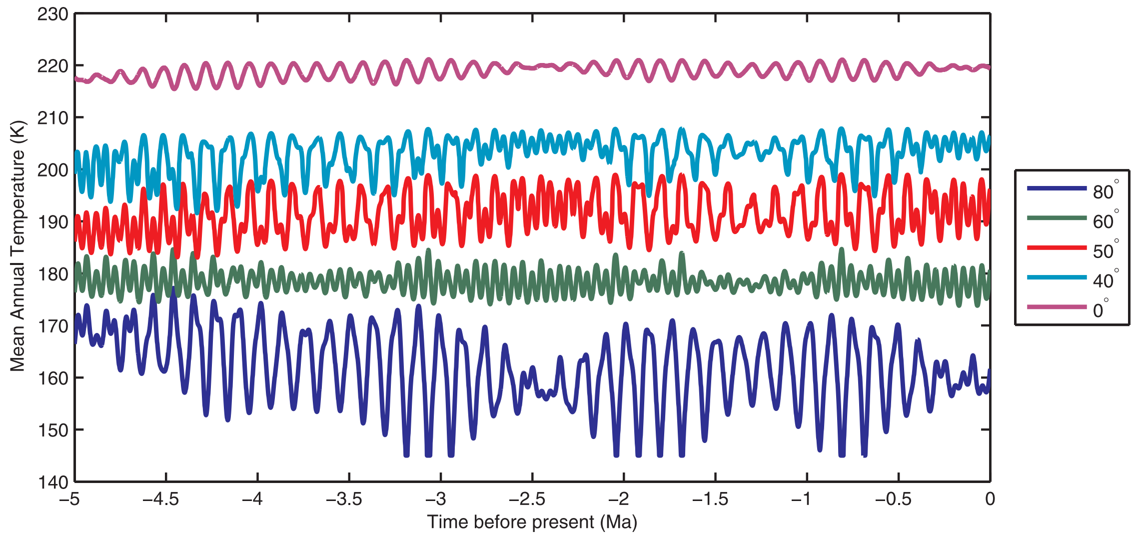

Figure 3. Annual mean surface temperature for several northern hemisphere latitudes. At 60°N the amplitude is relatively small and the main periodicity is shorter than at the other latitudes. These model calculations are for a uniform planet with a thermal inertia 220 J m^{-2}K^{-1}s$^{-1/2}$, an albedo of 0.2, and a 5 mbar CO_2 atmosphere.

change of variable, $dt/d\nu$, can be deduced from Kepler's second law. After some algebra one obtains

$$\overline{Q^{\frac{1}{4}}} = (S\sin\theta)^{1/4}\frac{1-e^2}{2\pi}\int_{-\omega}^{\pi-\omega}\frac{\sin^{1/4}(\nu+\omega)}{(1+e\cos\nu)^{3/2}}d\nu \tag{4}$$

$$= \frac{(S\sin\theta)^{\frac{1}{4}}}{2\sqrt{\pi}}\frac{\Gamma\left(\frac{5}{8}\right)}{\Gamma\left(\frac{9}{8}\right)}\left[1-\underbrace{\frac{12}{5}\left(\frac{\Gamma\left(\frac{9}{8}\right)}{\Gamma\left(\frac{5}{8}\right)}\right)^2}_{\approx 1.03} e\sin\omega + O\left(e^2\right)\right]. \tag{5}$$

Here Γ is the Gamma function. For comparison, the length of polar summer at the north pole is

$$\frac{P}{2}\left[1-\frac{4}{\pi}e\sin\omega + O\left(e^2\right)\right]. \tag{6}$$

Since $4/\pi \approx 1.3 > 1.03$, it is consistent to view the precession dependence of $\overline{Q^{1/4}}$ as a result of prolonged seasons. (Large powers of Q and peak insolation would have a precession dependence with the opposite sign [*Rubincam*, 2004; *Huybers*, 2006].) It also follows from equation (5) that

$$\frac{\frac{\partial\overline{Q^{1/4}}}{\partial(e\sin\omega)}\Delta(e\sin\omega)}{\frac{\partial\overline{Q^{1/4}}}{\partial\sin\theta}\Delta\sin\theta} \approx -4.1\sin\theta\frac{\Delta(e\sin\omega)}{\Delta\sin\theta} \approx -1, \tag{7}$$

given that the standard deviation of θ is about 5° and that of e sin ω is 0.05 over the last 3 Ma of Mars history. This estimate confirms that, at the north pole, precession is about as influential as obliquity changes.

[14] These two end-members represent planetary surfaces with infinite and zero thermal inertia respectively. For realistic thermal inertia, the surface temperature is neither constant nor equilibrates instantly with insolation, being intermediate between the two end-member cases. The relative importance of the orbital changes can be determined with Fourier power spectra or correlation coefficients. Both investigations lead to the same conclusions. It is clear that $\overline{Q}$ correlates strongly with obliquity, except at latitudes of ±45°, where it changes between positive and negative correlation. Figure 5a shows the correlations for $\overline{Q^{1/4}}$. As is clear from the foregoing discussion, most latitudes are controlled by precession. Figure 5b is for an airless uniform body in Mars orbit with I = 220 J m^{-2} K^{-1} s$^{-1/2}$ and A = 0.2; the annual mean temperature is controlled by obliquity, except around 62°–74° latitude where precession dominates. Eccentricity never plays the main role. If an atmosphere and seasonal CO_2 frost are added then this latitude

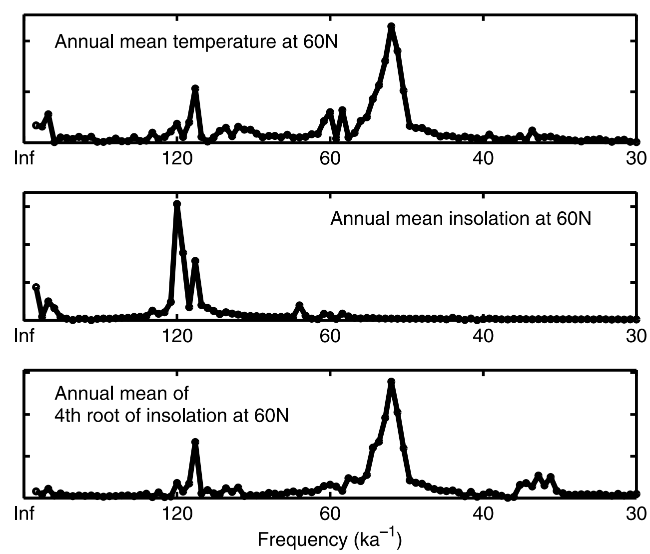

Figure 4. Fourier amplitudes of T_m, mean annual insolation, and the annual mean of the fourth root of insolation at 60°N from the last 3 Ma. The scale on the vertical axis is linear.

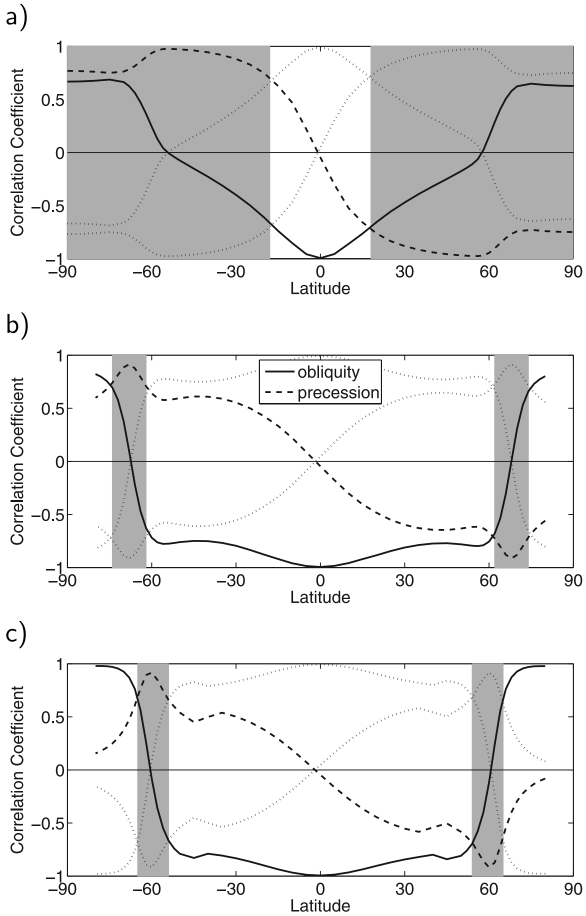

Figure 5. Correlation with orbital elements as a function of latitude for (a) $\overline{Q^{1/4}}$, (b) T_m of planet without atmosphere, and (c) T_m with atmosphere. The same thermal properties as in Figure 3 are used in Figures 5b and 5c. The dotted lines are the same data upside-down. Grey shaded areas indicate the latitude range where precession dominates over obliquity.

range shifts to about 54°–65° (Figure 5c). The same ranges are obtained from the analysis of Fourier power spectra.

[15] With T_m we have solved half of the Milankovitch problem for the extent of the permafrost layers; the other variable in equation (1) is T_f. Today the main source of water vapor in the martian atmosphere is known to be the north polar cap, but the history of the caps and atmospheric humidity are not reliably known. The humidity at mid-latitudes can be limited by supply or transport. If the former is the case, T_f changes far more than T_m in response to Milankovitch forcing, and T_f is likely controlled by obliquity, because of the large changes in polar summertime insolation it causes, although other possibilities have been raised. If the amount of water transported out of the polar regions is limited by a sluggish circulation, T_f might not have varied considerably over the last few million years; due to the small variation in T_m, the margin of the permafrost layers might have moved little, and the remaining variability would contain a significant precession dependence.

[16] The startling lesson in the context of the theory of terrestrial ice ages is how easily we could have gone wrong. Almost any other latitude and other moments of insolation than those pertinent would have led us to conclude that obliquity is the dominant driver.

[17] **Acknowledgments.** I thank Bruce Bills, Francois Forget, and Axel Timmermann for discussions. Model computations utilized the University of Hawaii Dell Cluster.

References

Boynton, W. V., et al. (2002), Distribution of hydrogen in the near-surface of Mars: evidence for subsurface ice deposits, *Science*, *297*(5578), 81–85.

Diez, B., et al. (2008), H layering in the top meter of Mars, *Icarus*, *196*(2), 409–421, doi:10.1016/j.icarus.2008.02.006.

Feldman, W. C., et al. (2002), Global distribution of neutrons from Mars: Results from Mars Odyssey, *Science*, *297*(5578), 75–78.

Forget, F., R. M. Haberle, F. Montmessin, B. Levrard, and J. W. Head (2006), Formation of glaciers on Mars by atmospheric precipitation at high obliquity, *Science*, *311*(5759), 368–371.

Huybers, P. (2006), Early Pleistocene glacial cycles and the integrated summer insolation forcing, *Science*, *313*, 508–511, doi:10.1126/science.1125249.

Imbrie, J., and K. P. Imbrie (1979), *Ice Ages: Solving the Mystery*, Harvard Univ. Press, Cambridge, Mass.

Kieffer, H. H., T. Z. Martin, A. R. Peterfreund, B. M. Jakosky, E. D. Miner, and F. D. Palluconi (1977), Thermal and albedo mapping of Mars during the Viking primary mission, *J. Geophys. Res.*, *82*, 4249–4291.

Laskar, J., B. Levrard, and J. F. Mustard (2002), Orbital forcing of the Martian polar layered deposits, *Nature*, *419*(6905), 375–377.

Laskar, J., A. C. M. Correia, M. Gastineau, F. Joutel, B. Levrard, and P. Robutel (2004), Long term evolution and chaotic diffusion of the insolation quantities of Mars, *Icarus*, *170*, 343–364.

Lebofsky, L. A., and J. R. Spencer (1990), Radiometry and thermal modeling of asteroids, in *Asteroids II*, edited by R. P. Binzel, T. Gehrels, and M. S. Matthews, pp. 128–147, Univ. of Ariz. Press, Tucson.

Leighton, R. B., and B. C. Murray (1966), Behavior of carbon dioxide and other volatiles on Mars, *Science*, *153*, 136–144.

Mellon, M. T., and B. M. Jakosky (1993), Geographic variations in the thermal and diffusive stability of ground ice on Mars, *J. Geophys. Res.*, *98*(E2), 3345–3364.

Mellon, M. T., W. C. Feldman, and T. H. Prettyman (2004), The presence and stability of ground ice in the southern hemisphere of Mars, *Icarus*, *169*, 324–340, doi:10.1016/j.icarus.2003.10.022.

Mitrofanov, I. G., et al. (2002), Maps of subsurface hydrogen from the high-energy neutron detector, Mars Odyssey, *Science*, *297*(5578), 78–81.

Murray, B. C., W. R. Ward, and S. C. Yeung (1973), Periodic insolation variations on Mars, *Science*, *180*, 638–640.

Rubincam, D. P. (2004), Black body temperature, orbital elements, the Milankovitch precession index, and the Seversmith psychroterms, *Theor. Appl. Climatol.*, *79*, 111–131.

Schorghofer, N. (2007a), Theory of ground ice stability in sublimation environments, *Phys. Rev. E*, *75*, 041201, doi:10.1103/PhysRevE.75.041201.

Schorghofer, N. (2007b), Dynamics of ice ages on Mars, *Nature*, *449*(7159), 192–194, doi:10.1038/nature06082.

Schorghofer, N., and O. Aharonson (2005), Stability and exchange of subsurface ice on Mars, *J. Geophys. Res.*, *110*, E05003, doi:10.1029/2004JE002350.

Toon, O. B., J. B. Pollack, W. Ward, J. A. Burns, and K. Bilski (1980), The astronomical theory of climate change on Mars, *Icarus*, *44*, 552–607.

Touma, J., and J. Wisdom (1993), The chaotic obliquity of Mars, *Science*, *259*, 1294–1297.

van Hemelrijck, E. (1983), The effect of orbital element variations on the mean seasonal daily insolation on Mars, *Moon Planets*, *28*, 125–136.

Ward, W. R. (1974), Climatic variations on Mars: 1. Astronomical theory of insolation, *J. Geophys. Res.*, *79*, 3375–3386.

Ward, W. R. (1979), Present obliquity oscillations of Mars: Fourth-order accuracy in orbital *e* and *I*, *J. Geophys. Res.*, *84*, 237–241.

Ward, W. R. (1992), Long-term orbital and spin dynamics of Mars, in *Mars*, edited by H. H. Kieffer et al., chap. 9, pp. 298–320, Univ. of Ariz. Press, Tucson.

N. Schorghofer, Institute for Astronomy, University of Hawaii at Manoa, 2680 Woodlawn Drive, Honolulu, HI 96822, USA. (norbert@hawaii.edu)